Silicon (2022) 14:1617–1627
https://doi.org/10.1007/s12633-021-00944-5

ORIGINAL PAPER

Influence of SiC Particles on Mechanical and Microstructural Properties of Modified Interlock Friction Stir Weld Lap Joint for Automotive Grade Aluminium Alloy

V. Paranthaman [1] · K. Shanmuga Sundaram [2] · L Natrayan [2]

Received: 10 October 2020 / Accepted: 5 January 2021 / Published online: 4 February 2021

Abstract
The present requirement of the aerospace industry is seeking light-weight joining material that satisfies the technical and technological requirements with better mechanical characteristics. Aluminum alloy with spot-welding process meet the requirements of modern demands. In this present paper, a modified-interlock friction stir weld lap joint is induced to join AA8011-AA7475 with different wt% of SiC particles. Friction stir machine process parameters were tool rotational speed 1600 rpm, plunge speed rate 0.08 mm/s and traverse speed 40 mm/s maintained constantly. Mechanical and metallurgical characterizations were investigated. EDS analysis and microstructure confirmed the presence of silica particles in the NZ of the weld joints and uniformed homogenous distribution of the particulates throughout the weld. Joints made with SiC particulates showed improved static properties because intensive softening occurred in the stir zone leading to Si-Al-based precipitate particulates. The fracture test showed that the joints with SiC had a ductile fracture. AA8011-AA7475 with 2 wt% SiC showed maximum hardness, tensile strength of 229 HV, 192 MPa and a decrease in elongation was observed from 9.5 to 5%. AA8011-AA7475/2 wt% showed improved hardness, tensile strength and elongation suitable for aircraft wing stringers application.

Keywords Aluminium dissimilar joining · Friction stir lap welding · Interlock joint · Fractography · Mechanical properties

1 Introduction

Friction stir welding has to gain significant attention among the researchers as the preferable joining technique for welding of monolithic materials and metal matrix composites [1]. **Compare to the conventional welding, dissimilar welding technique produce less heat, reducing internal stress and forms the intermetallic compounds.** The FSW tool pierces the surface of weld sheets to perform the fusion of sheets. Navaneet Kanna et al. made a novel study on AA 6061-T6 and AA8011-h14 dissimilar inferring that the maximum tensile strength of 77.08% is obtained at AA 8011 placed on the advancing side rather than the retreating side [2]. K. Palani et al. investigated the mechanical properties and microstructural characteristics of AA 8011 H24 -AA 6061 T6 with Al_2O_3 and SiC nanoparticles. Dissimilar joints in Nugget Zone found the better shear strength and microstructural features of the joints made with SiC showed uniform distributions [3]. P.Chandrasekar et al. investigated the effects of carbide reinforcements on similar AA8011. Results show that 8 wt.% B_4C reinforcement increased the hardness and tensile strength for the composite sheet due to uniform distribution and grain refinement [4]. The fatigue characteristics of dissimilar friction stir welded stainless steel used in vehicles as valve material was analysed. Investigation shows the fatigue life of the welded surface was high. Dissimilar friction stir welded stainless steels were widely used in various engineering fields [5]. **Higher mechanical strength weld joints obtained with the friction force, because it helps break up the oxide layer and provides the enhanced material flow and mixing by inducing severe plastic deformation** [6]. Jacquin et al. survey show the latest research and applications of the FSW process, the automation and its control in the field of aerospace, automotive, and shipbuilding [7]**.** Prater T et al. reported that the welding pin tool's wear due to prolonged contact

✉ V. Paranthaman
paranthphd@gmail.com

[1] Department of Mechanical Engineering, Adhi College of Engineering and Technology, Chennai, India

[2] Department of Mechanical Engineering, Anna University, Chennai, India

with the MMCs was examined using tools made of steel, cemented carbide uncoated, and coated with diamond. The diamond coatings enhanced tool strength with reduced wear rate during FSW [8]. Ranpan et al. explored the cold rolling influence of residual stress on AA7475 alloy and deduced that there is a uniform distribution of residual stress throughout the nugget zone of the welds reducing the magnitude of residual stress in the core area of the welded material [9]. **The weld interfaces material flow was observed to decrease with the increase in plunge speeds, which dented the weld strength. Increased plunge depth during FSW resulted in better material interaction at the weld interface to increase the joint strength. The FSW process improves significantly on the strength, fatigue and fracture stiffness of the weld made by the FSW process compared to traditional fusion welding techniques** [10]. Martin Kadlec et al. studied the mechanical behaviour of AA7475 friction stir welds with the kissing bonds and established that the kissing bond with the critical size of 670 μm has a huge influence on the statistical properties and microstructure characteristics of the joints [11]. However, the size of the kissing bond does not influence the weld characteristics. Storjohann et al. reported FSW process does not melt the workpiece, and temperatures reach up to 90% of the melting point. Some of the researchers hypothesized the presence of smaller concentrations of Aluminium Carbide phases in the weld region[12]. Kim et al. (2006) reported that the high temperature could alter Si particle size. The alignment of SiC particles in each stir zone is different from that of other weld zones[13]. SiC addition to aluminum alloys offered good tensile strength [14], hardness, density and wear resistance [15]. Senthil Kumar et al. reported SiC particles size 10 μm showed better results than 20 μm and 40 μm [16]. Previous research works reveal that reinforcing particles is a more significant influence to increase/decrease the mechanical properties of weld joints. Many authors reported on the FSW lap joint with reinforcement particles not finely dissolve in the nugget zone. Moreover, there is no literature available on investigating the mechanical properties of AA8011-AA7475 dissimilar alloy. In this research, a novel modified interlock friction stir weld lap joint used to study the effects of SiC reinforcement in AA 8011-AA7475 dissimilar alloy. The mechanical properties such as hardness, tensile strength, elongation, microstructure, and fractography properties were investigated.

2 Experimental Procedure

FSW interlock dissimilar lap joints AA8011-AA7475 having 3 mm thickness integrating SiC with various wt percentage (0 to 5 wt%) of 10 μm average particle size were performed in this experimental work [16]. AA8011-AA7475 dissimilar alloy widely used in aircraft wing stringers application. Table 1 shows the aluminium sheet metal composition. The sheet sizes of 150 mm × 100 mm × 3 mm were used for performing the hybrid interlock lap joints.

Table 1 Base metals chemical composition

Base metal	Si	Cu	Mg	Zn	Ti	Fe	Cr	Mn	Al
AA 8011	0.12	2.3	2.3	5.9	0.03	0.15	0.03	0.5	88
AA 7475	0.04	1.5	2.3	5.7	0.06	0.12	0.22	0.06	90

Before performing the weld, oxide layers are removed from weld sheets and cleaned well with cleansing agents to eliminate the rust particles in the aluminium surface[17]. The aluminium sheets were milled to a pitch of 0.5 mm and a width of 30 mm from the centre of the aluminium sheet. The work sample mounted on top is milled to 0.5 mm wide that interlocks with the un-machined bottom sample to form a hybrid lock between the welds**. A groove of 0.5 mm depth and 10 mm widh is milled on aluminium plate at the bottom for filling SiC particles**. Figure 1 displays the graphical representation of the modified interlock lap joint.

A cylindrical pin tool is used for joining the interlock joints. The shoulder diameter, length, and diameter of the pin is 25 mm, 4 mm, and 5 mm, respectively. **Silicon carbiate chemical composition showed in** Table 2**.** Figure 2 shows the microstructure images of SiC particulates used in modified lap joints.

Modified Interlock AA8011-AA7475 dissimilar aluminum sheet showed in Fig. 3. The process factors used for welding are 1600 rpm of rotational tool speed, 40 mm/s of traverse speed, and 0.08 mm/s of plunge speed rate. **The distance plunged by the tool into the work material were considered 2.7 mm (plunge depth) in this study.** Table 3 indicates the sample code and composition wt% considered in this experiment. Figure 4 (a–f) represents the hybrid joints incorporating SiC. **Micro-hardness of FSW lap weld samples was measured using the Vickers digital micro-hardness tester under the standard load of 0.05 Kg for the duration of 15 s. Hardness was measured five different points in the weld sample nugget zone.** Figure 5 exposed the dimension of the tensile test sample. The tensile test samples are cut under standard ASME D8.9–97 and measured at 0.5 mm/min cross-head speed in Shimadzu universal testing machine[18].

3 Results and Discussion

3.1 Vickers Hardness Test

Figure 6 depicts Vickers hardness with various wt% of SiC particulates at tool speed of 1600 rpm, traverse speed of 40 mm/s, plunge speed rate of 0.08 mm/s, respectively. Apart from process

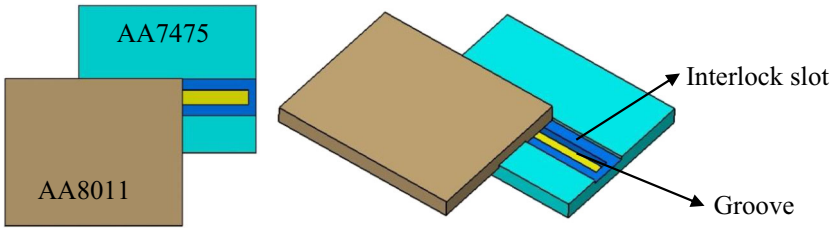

Fig. 1 Modified interlock lap joints graphic representation

parameter factors, the SiC particulates have a major influence in softening the SZ of welds due to fine granules in the SiC particulates [19]. Silica particulates prevent the dislocation movement in the Si-Al matrix. Hence, It has reduced the deformation and penetration at cutting area of the weld surface [20]. The various combinations of SiC particulates impact the hardness of welds to a considerable level [21]. Increase the SiC particulates wt% in weld joints from 2% to 5% greatly influences the hardness and a gradual decrease when the SiC wt% is increased beyond certain wt%. Si particles have a more significant effect on the hardness of the interlock joints. The joints with 2 wt% of SiC particulates (sample 3) showed high hardness value among various wt% incorporated in weld joints. FSW interlock joint AA8011-AA7475 with 2 wt% SiC showed a high hardness value of 229 HV. Increasing the SiC wt% over certain limit particle clustering occurred on the weld sample. It has increased the plasticizing ability and density dislocation reduces the hardness [22].

The higher hardness value was found with 2% wt SiC due to hard silica particulates and greater mixing ability of SiC to mix with the nugget zone of the welded joints. Because silica particles in the aluminium alloy protect the softer matrix and obstacles to the movement of dislocation. Thus, limiting the deformation and resists the penetration and cutting of slides on the welded joints surface. It was also noted that the addition of more than 2 wt% of SiC results in a significant increase in the bulk hardness of aluminium alloy, which makes the interlock welded joints more brittle in nature. Hence, modified interlock lap welds hardness result showed that 2 wt% SiC particulates considerably increase the weld joints hardness. Modified interlock weld joint sample 3 hardness increased by 23% than AA8011-AA7475 dissimilar base metal.

3.2 Hardness Profile of FSW Modified Lap Welds AA 8011-AA7475 /SiC

Figure 7 **shows the FSW lap weld joints typical hardness profile with 2 wt% of SiC particulates. It can be concluded that the profile of the welding joints is based on different wt% of the SiC particles.** The microstructure changes based on the mechanisms used to soften SZ in the weld of strength and size of the grain particulates [23]. SiC particulates increased the shear strength of welds due to the transfer of stress from alloy-SiC. The bonding in-between the grain dislocations and particulates improve the strength of the welds.

Particulates are the primary factor for deciding the statistical characteristics of AA 8011-AA 7475 weld joints. The hard and brittle SiC particulates lead to dispersion within the Al-Si interface. The particulates form a binary stage in the surrounding substance and withstand dislocation movements in the hybrid interlock joints. The weld joints hardness related to the wt% of particulates, although a notable effect is absent in HAZ/TMAZ [24]. **The silica particulates mix thoroughly in SZ of the hybrid welds in hardening particulates due to refined silica grains in particulates chosen as the interlayer.** Figure 7 **exposed that hardness is minimal in the TMAZ region, as wt% of SiC particulates is gradually increased. Thus, the hardness of welds with 2% wt SiC particulates showed higher hardness values than the other wt% of SiC at the weld zone of interlock welds** (Fig. 6).

3.3 Mechanical Properties of Modified Interlock FSW Lap Welds

The hybrid interlock welds made using 2% wt SiC has the highest tensile strength of 192 Mpa. Apart from 2% wt SiC,

Table 2 Chemical composition of SiC particles

Elements	SiC	Si	SiO_2	Fe	Al	C
Percentage	98.5	0.3	0.5	0.08	0.1	0.3

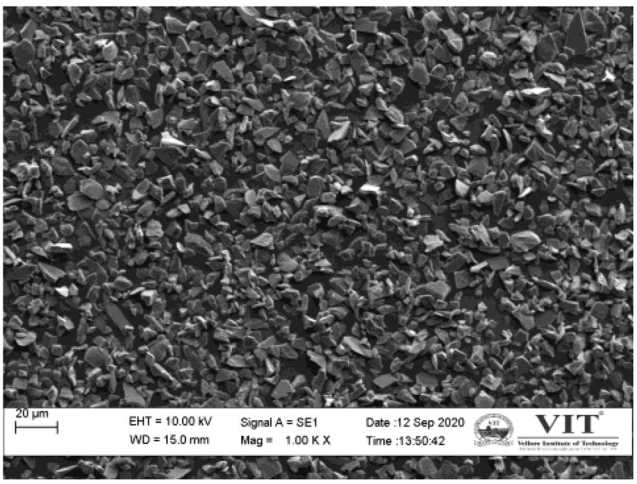

Fig. 2 SEM of SiC particulates

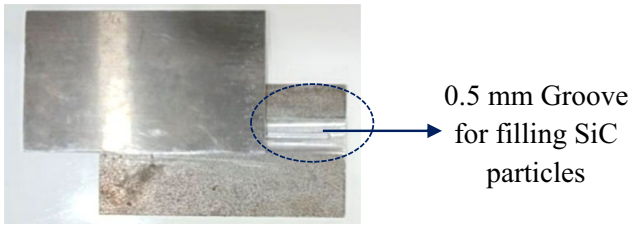

Fig. 3 Modified interlock AA8011-AA7475 dissimilar aluminum sheet

fewer deviations in tensile strength values were obtained for other wt% of particulates [25]. However, higher tensile strength with 2% wt SiC is due to the even distribution of particulates throughout the SZ region of hybrid interlock joints. Thus, uniform distribution at the weld zone and the distribution of particulates placed in-between aluminium sheet is caused by the FSW tool at high speeds.

The other welds with (1%, 3%, 4%, 5% with SiC) exhibit slightly low values of tensile strength because of the influence of SiC particulates wt%. While interlayer particulates wt% increased beyond 3%, the shrinkage defect occurs on the surface of the aluminium alloys; Shrinkage defect reduces the weld joints strength [26]. The wt% of particulates beyond 3% induces the keyhole and uneven mixing of particulates in the weld joints due to varying wt% of the particulates. The SiC reinforcement penetrates the stir zone of base metal and avoids crack formation in which silica prevents crack propagation [27]. Therefore, the microstructure exhibit reinforcement in the stir SZ has an enormous influence on the joining of modified lap joints as represented in Fig. 10 (b). An equal amount of SiC particulates mixes well in the TMAZ/HAZ and eliminates crack propagation (Fig. 10c). Frequent crack path occurs in the nugget zone of FSW modified lap joints since grain coarsening and dissolution of reinforcement particulates occur between lap joints due to various volume fractions of the reinforcement particulates. In the welds with 1% SiC, the fracture occurs in the SZ since lower wt% of SiC incorporated in between the dissimilar aluminium sheets. The weld pattern of lap welds with 4% and 5% wt of the particulates forms shrinkage patterns due to increased volume fractions of silica content[28]. Modified interlock welds with higher wt% of particulates have coarse precipitates with

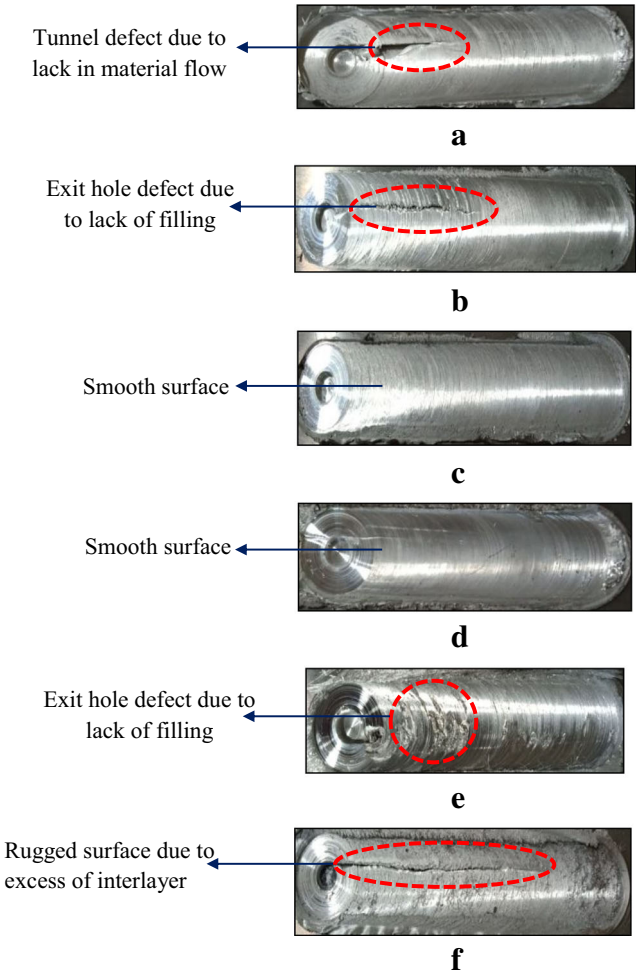

Fig. 4 FSW Interlock welds with different wt% of SiC reinforcements. (**a**) Sample 1 (AA8011-AA7475 Base metal), (**b**) Sample 2 (AA8011-AA7475/1 wt% SiC), (**c**) Sample 3 (AA8011-AA7475/2 wt% SiC), (**d**) Sample 4 (AA8011-AA7475/3 wt% SiC), (**e**) Sample 5 (AA8011-AA7475/4 wt% SiC), (**f**) Sample 6 (AA8011-AA7475/5 wt% SiC)

fine dimples on the weld surface since fracture occurs under heterogeneous conditions [29]. Modified interlock welds joints with SiC reinforced fractures along the leading edge of the weld. The welds fractured in the progressing sides show that the welds are strong adequate to resist the shear strength because of hard silica particulates engaged in the weld sample.

Table 3 Weld samples and particulates wt%

Sample code	Composition
Sample 1	AA AA8011-AA7475
Sample 2	AA8011-AA7475/1 wt% SiC
Sample 3	AA8011-AA7475/2 wt% SiC
Sample 4	AA8011-AA7475/3 wt% SiC
Sample 5	AA8011-AA7475/4 wt% SiC
Sample 6	AA8011-AA7475/5 wt% SiC

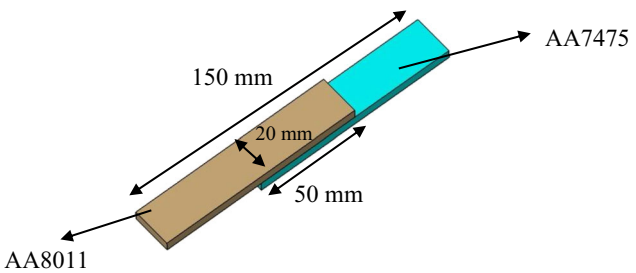

Fig. 5 Tensile specimen (ASME D8.9–97 standard)

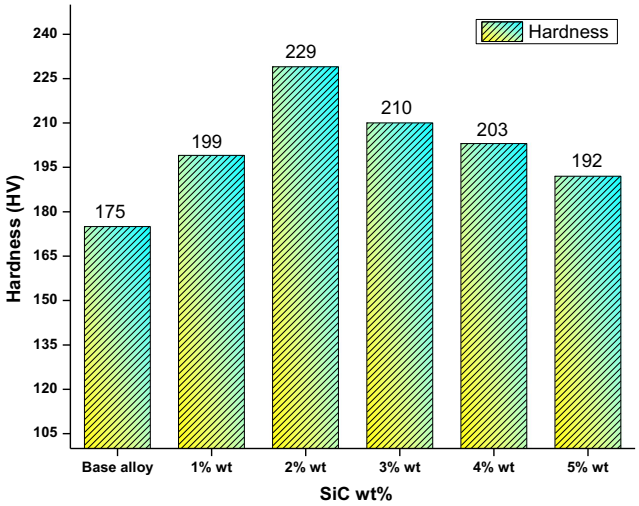

Fig. 6 Vickers hardness for different wt% of modified interlock weld joints

3.4 Effect of SiC on Tensile Properties of FSW Modified Lap Joints

Figure 8 (a) represents the ultimate tensile strength of hybrid FSW lap welds with various wt% of SiC particulates. AA8011-AA7475 with 2 wt% of SiC particulates (sample 3) showed a high tensile strength of 192 MPa among various wt% incorporated in weld joints. Modified interlock weld joint sample 3 tensile strength was increased by 12.5% than AA8011-AA7475 dissimilar base metal. Figure 8 (b) exposed the elongation percentage of modified FSW lap welds with various wt% of SiC particulates. The elongation percentage of reinforced weld joint is reduced due to the formation of refined grains and fragmentation of reinforcement particles in the weld zone. The elongation of 2 wt% hybrid interlock joints showed low value. Figure 8 (c) showed the engineering stress and engineering strain curve for sample 1 and sample 3. Results exposed that AA8011-AA7475 with 2 wt% SiC joints showed better elongation then AA8011-AA7475 dissimilar base metal. Figure 8 (d) shows the maximum force obtained in the area of the weld. All interlock welds with reinforcements are rigid enough to withstand the transverse force acting on the weld region [28]. Weld zone maximum force observed 31,548 N (sample 3). The substantial improvement in the static properties of SiC lap joints is due to the uniform SiC distribution in the welds stir zone.

Modified interlock FSW with SiC represented better strength for the aerospace application in welds produced. Adequate strength was observed in the SiC weld joints to withstand the force with required wt% and fracture detected away from the stir zone of joints [30]. Md Aleem pasha et al. tested AA6061 joints properties and suggested that the SiC reinforced welds have greater strength and statistical values than the base material [31]. F.J. Humphreys et al. proposed that the dislocation decreases and subsequently reinforcements pile up at grain boundaries since SiC particulates have a significant effect on hybrid interlock joints [32].

The Onion rings obtained with good and week strength SiC reinforced joints in the NZ of the FSW modified lap welds are shown in Fig. 9 (a, b). The regions in the macrostructure represent the thoroughly mixed reinforcements in the nugget zone. The well-structured onion rings are formed due to the deposition layer of SiC particulates.

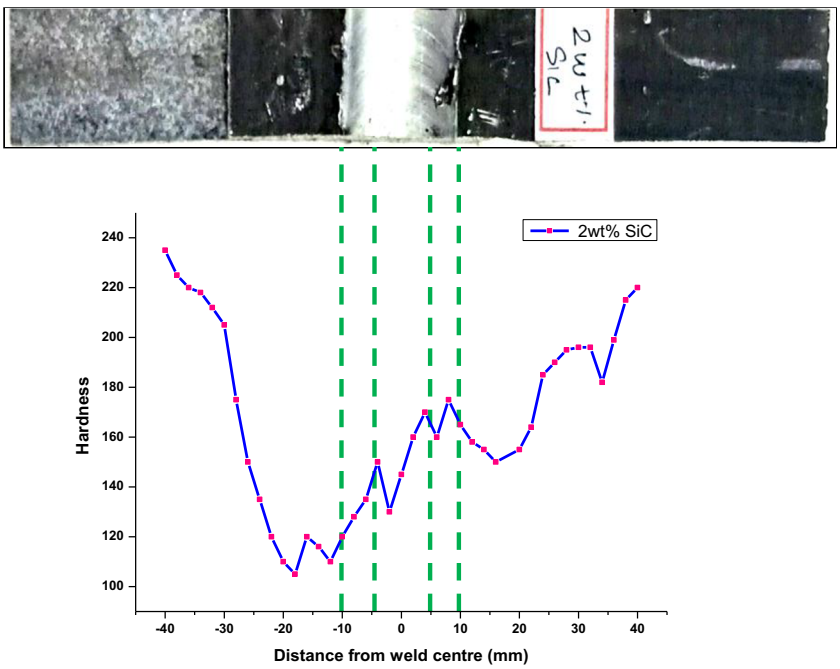

Fig. 7 "W" shaped hardness of FSW interlock lap joints with 2% SiC

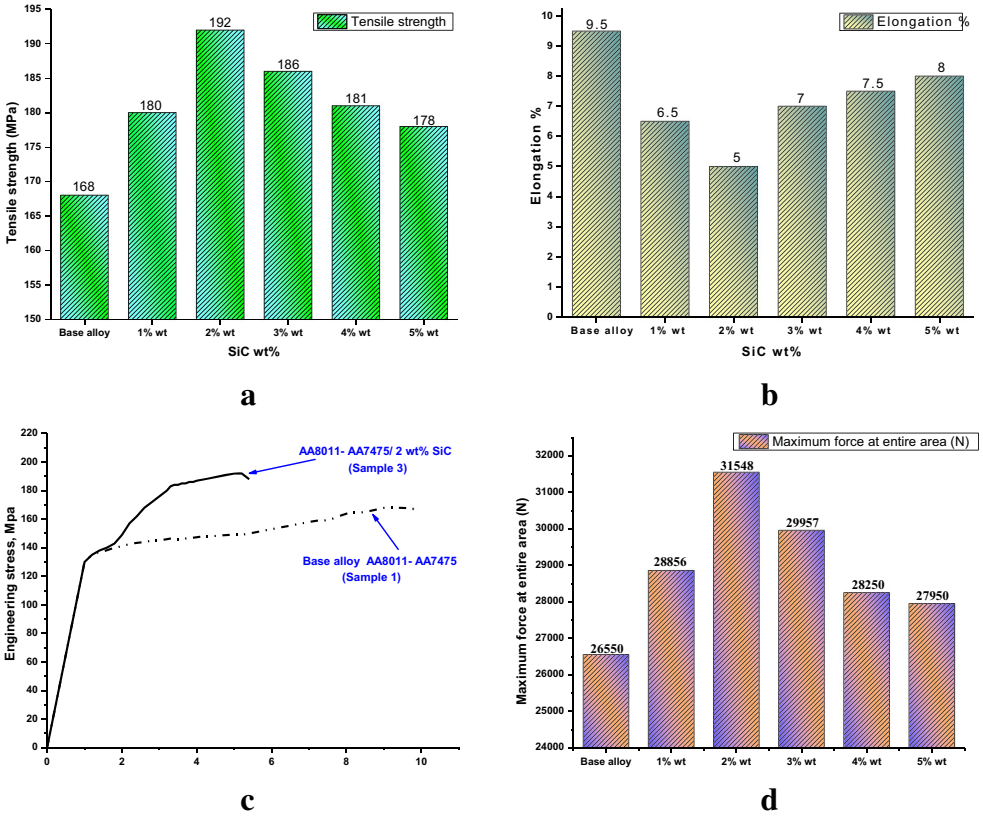

Fig. 8 (**a**) Tensile strength, (**b**) Elongation %, (**c**) Stress and strain curves for S1 and S3, (d) Maximum force at weld region

3.5 Microstructure of SiC Incorporated FSW Lap Welds

The optical transverse section micrographs of interlock dissimilar weld from different weld zones regions are depicted in Fig. 10. The microstructure of interlock friction stir joints is sub-divided into four regions such as base material (BM), welded nugget zone (WNZ), heat-affected zone (HAZ), thermo-mechanical affected zone (TMAZ). The microstructure of interlock friction stir joints exhibits typical characteristics. The base material microstructure confirms that the aluminum alloy comprises elongated grains and fine IMC [33]. In interlock welded joints, aluminium alloys microstructure after joining remains invariant due to relatively low temperature and the negligible pressure during the welding process. Figure 10 (a) relates to the weld nugget zone with fine grains obtained by dynamic recrystallization (DRX) because of dissimilar alloy stirring that occurs while rotating the pin tool. Figure 10 (b) depicts the uniform particle distribution in the WNZ. Figure 10 (c) represents the interlock weld joints' microstructure in 4 wt% SiC of the welds along the boundary of WNZ and TMAZ of advancing and retreating sides of the welds. Apart from this, the high SiC wt% promotes the formation of merged grain structures and agglomerated SiC particles at TMAZ and WNZ in the interlock weld joints[34]**.** TMAZs grain much greater than the WNZ grains and flows upwards between the interlock lap joints. During the FSW welding, materials in the weld zone experience plastic deformation due to the extruder impact from the WNZ by the

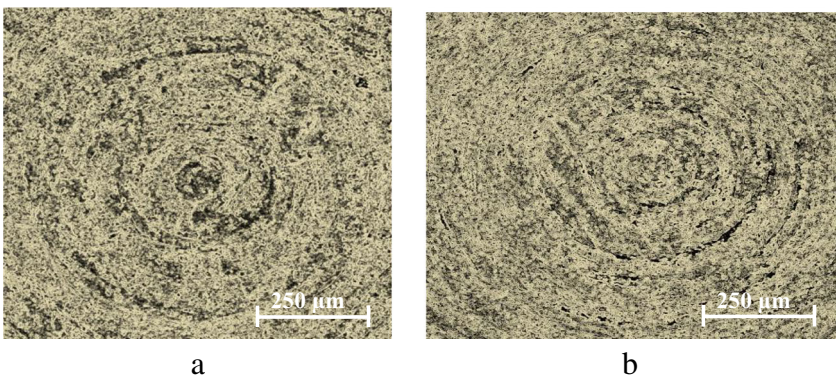

Fig. 9 Macrostructure of FSW interlock lap joint at the stir zone incorporating SiC particulates. (**a**) AA8011-AA7475/2wt%SiC (Sample 3), (**b**) AA8011-AA7475/5wt%SiC (Sample 6)

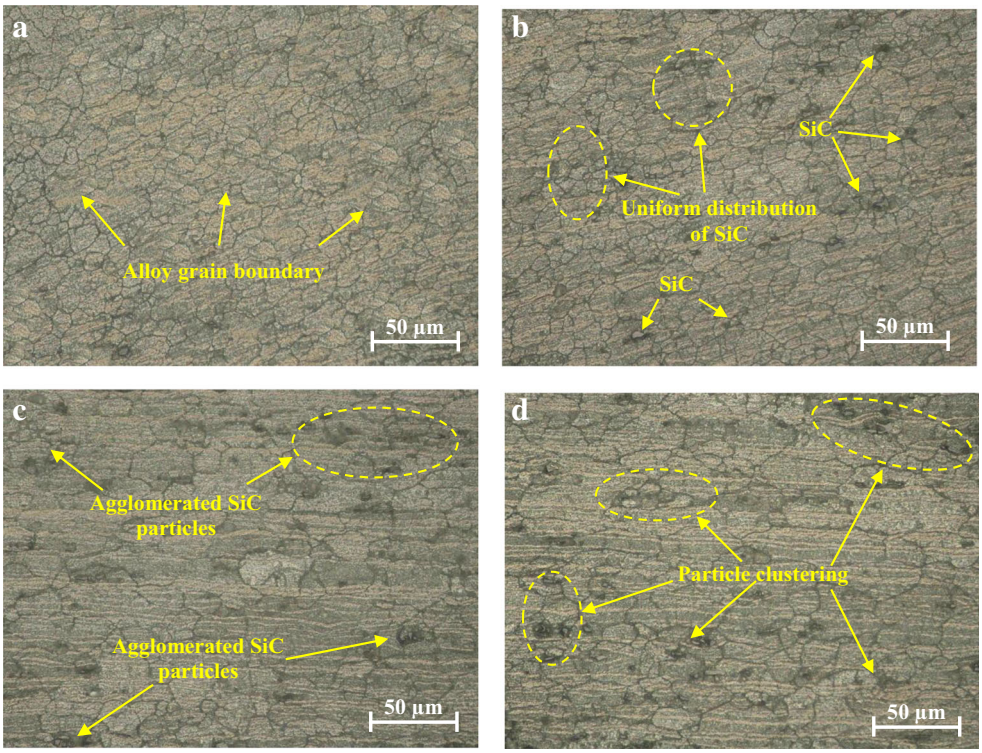

Fig. 10 Micrographs of FSW modified lap welds with different particulates wt%. (**a**) AA8011-AA7475 (Sample 1), (**b**) AA8011-AA7475/2wt%SiC (Sample 3), (**c**) AA8011-AA7475/4 wt% SiC (Sample 5), (**d**) AA8011-AA7475/5 wt% SiC (Sample 6)

rotating shoulder. The heat-affected zone (HAZ) is referred to in Fig. 10 (d), where the grain size is greater than the base metal.

The particle clustering in the weld region was coarser due to the high wt% SiC in this region deters plastic deformation leading to the formation of elongated and piled up grains in the weld nugget zone [4]. For the base metal AA 8011, the Al-Mg-Si system, the main strengthening phase is plate-shaped β with a CFC structure, while the strengthening phase of AA 7475 is the Al-Mg-Cu system[35]. It can be noted that the areas across the dashed line on the right side show distinct morphology while on the left side, the second phase particles are smaller in size than on the other side due to pin geometry employed during the FSW process. This phenomenon could be due to different particle sizes of the base materials in the second phase caused by different alloy elements in AA 8011 and AA 7475.

3.6 Fractography of SiC Incorporated FSW Lap Welds

The fracture of weld specimens determines the ductile character of the hybrid interlock joints. Figure 11(a) exposed low plastic deformation due to slight dimples. It has mainly localized at the boundary between broad dimples and ductile crack of the structure. Figure 11 (b–d) depicts the SEM of fractured FSW joints with SiC reinforcements. It exposed challenging to detect any significant difference in dimple structure on fracture samples due to the SiC particle distribution throughout the dimple-dominated zones. The welds with 1% wt reinforcement particulates have limited dimples and pores than joints made with 5 wt% as shown in Fig. 11(b).

Fracture locations of hybrid FSW joints with SiC particulates represent small pores and dimples represent the ductility of FSW joints[36]. Fractured joints with 2 wt% SiC have fine pores on the joints with SiC depicting an extraordinary bond between particulates and welds in the SZ as shown in Fig. 11(c). SiC particulates are evenly spread on aluminium sheet grain boundaries due to silica enhancing the ductility of weld joints [37]. Figure 11(d) shows coarser dimples in the FSW lap joints region because of the existence of SiC content. Higher wt% particles welds show coarse and broad dimples with coarse precipitation. The fractured structure is very dense in sample 3. The equivalent wt% of SiC undergoes an adequate generation of heat for grain recrystallization in the nugget zone of joints and thereby the SiC particulate distribution is homogenous. Thus, welds with SiC have higher statistical properties irrespective of weight percent of the reinforcements.

AA8011-AA7475 dissimilar base metal (Sample 1) and AA8011-AA7475/2 wt% SiC (sample 3) EDS analyses exposed in Fig. 12 (a) and (b). Figure 12 (a) exposed that high Al, and presence of Cu, Mg, Zn, C, O elements conformed in sample 1. AA8011-AA7475 dissimilar base metal EDS results shows 3.34 wt% O, 1.32 wt% C, 2.05 wt% Cu, 2.13 wt% Mg, 2.90 wt of Zn and 88.87 wt% of Al. The oxide observed as a major secondary element in sample 1. Figure 12 (b) EDS results shows that Al, Si, Cu, Mg, Zn, C and Oxide

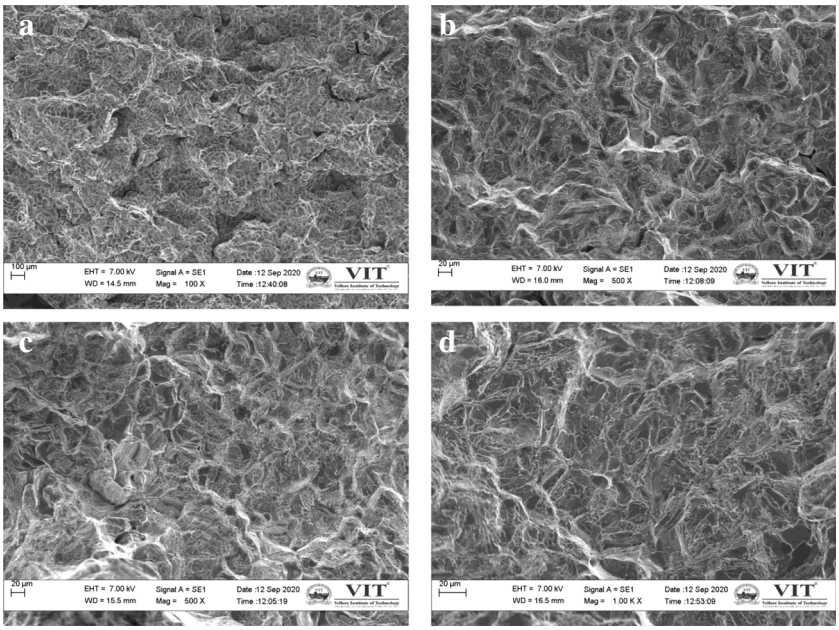

Fig. 11 Fractography of reinforced FSW modified joints with SiC. (**a**) AA8011-AA7475 (Sample 1), (**b**) AA8011-AA7475/ 1 wt% SiC (Sample 2), (**c**) AA8011-AA7475/ 2 wt% SiC (Sample 3) (**d**) AA8011-AA7475/5 wt% SiC (Sample 6)

are elements of weld sample on the fracture surface. Sample 3 fracture surface shown that negligible oxides and silica composition predominant. Fracture surface study revealed that free microcracks and dimples in the samples due to the uniform distribution of SiC particles. The presence of silica improves the mechanical properties significantly in the weld sample.

In order to understand the interlayer particle distribution, sample 1 (base metal) and sample 3 (Interlock weld sample) were considered to carry out the electron backscattered diffraction (EBSD) analysis. Base metal such as AA8011 (Fig. 13 a) and AA7475 (Fig. 13 b) EBSD results exposed large grain size of 36.55 µm, 32.44 µm and permanent distortion intensity varied among the modified lap joints. Figure 13 (c) exposed SiC reinforced interlock joints with the formation of partly uniform average grain size 7.55 µm then base alloys grain structure (Fig. 13 a, b). Because of continuous dynamic recrystallization (CDRX) and severe plastic deformation (SPD) occurs in the south zone. It acted an obstacle to the movement of grains and delayed the grain development via the Zener-pinning mechanism. High permanent distortion is detected in the bottom sheet due to

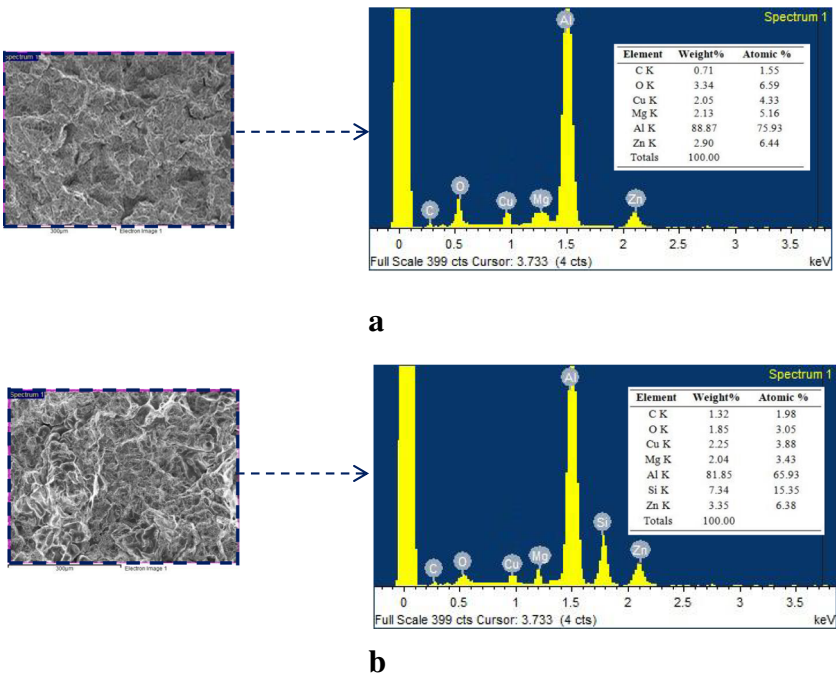

Fig. 12 (**a**) EDS analysis for Sample 1 (AA8011-AA7475 dissimilar base metal). (**b**) EDS analyses for Sample 3 (AA8011-AA7475/2 wt% SiC)

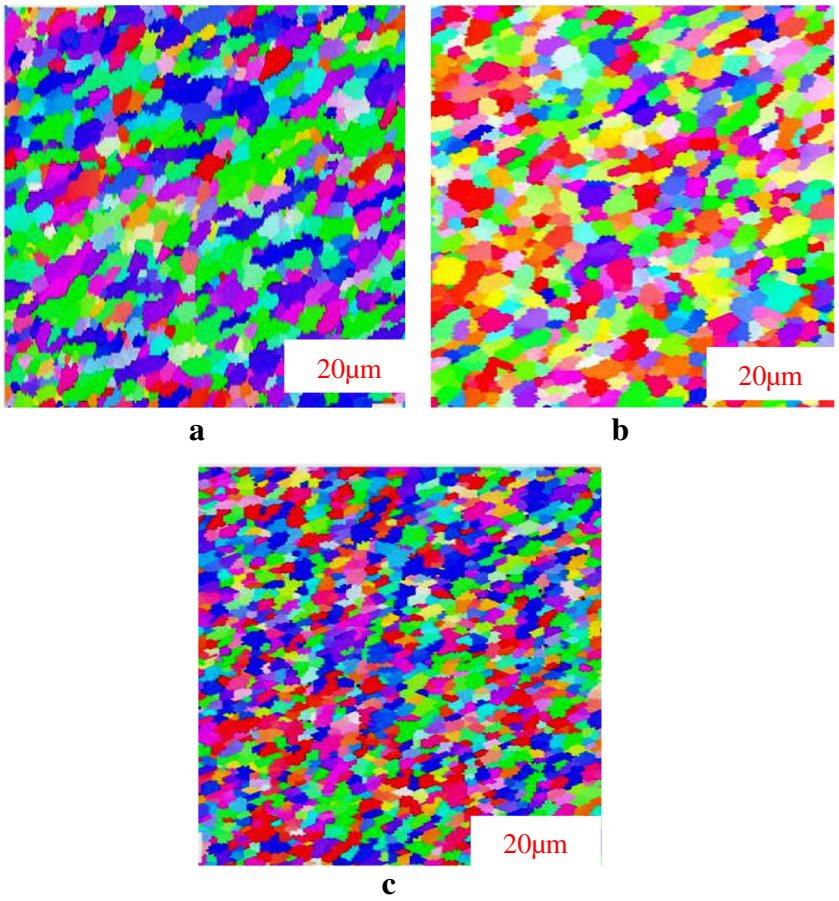

Fig. 13 EBSD structure of grain distribution. (**a**) AA8011 (Base metal), (**b**) AA7475 (Base metal), (**c**) AA8011/AA7475/2 wt% SiC (sample 3)

fine SiC particles influence during FSW welding. Fine-grain was formed in the north zone because of the existence of silica elements in the stir region.

4 Conclusion

AA 8011-AA7475 with different wt% of SiC reinforcement on modified interlock lap joints successfully welded through friction stir welding. The samples were characterized and drawn the following conclusions:

- **AA 8011-AA7475/2 wt% SiC (sample 3) showed maximum hardness, tensile strength and elongation of 229 HV, 192 MPa and 5% respectively.**
- **Incorporating SiC in the modified interlock lap welds plays a crucial role in the stir zone as the fine particulates in SiC mix thoroughly for piling-up and nucleating the grain structures.**
- **W-shaped hardness profile revealed that sample 3 weld had withstood the shear force. The presence of SiC particulates influences welds strength and their grains structure provides the obstructing dislocation movements.**
- **Microstructure results conclude that onion ring formation with refined grains in SZ showed higher lap strength. The improvement in the statistical properties of weld joints with SiC is due to the refinement of grains in the stir zone due to the FSW tool's high rotation speed.**
- **The fracture of weld specimens determines the ductile character of the hybrid interlock joints.**
- **AA 8011-AA7475/2 wt% SiC hardness and tensile strength improved by 23%, 12.5% then dissimilar AA 8011-AA7475 base metal.**

This study claims that AA 8011-AA7475/2 wt% SiC significantly enhanced the hardness and tensile strength properties. Therefore, it can be concluded that using SiC as reinforcement stands as the best-suited with characteristics in the application of aircraft wing stringers to meet the modern demands of the aerospace industries.

Acknowledgments The authors thank Kathiravan Metal Bellows India Private Limited for its financial assistance.

Author Contributions *V. Paranthaman*: Supervision, Investigation, Writing- Reviewing and Editing.
K. Shanmuga Sundaram: Software, Writing, Supervision, Editing.
Natrayan L: Conceptualization, Investigation, Methodology, Software.

Funding This work is supported by the "Innovation research and development fund, Kathiravan Metal Bellows India Private Limited – Chennai" grant number IR&D/0026/CH-011/2019.

Data Availability The datasets analyzed during the current study are available from the corresponding author on reasonable request.

Compliance with Ethical Standards

This article does not contain any studies with human participants or animals performed by any of the authors.

Conflict of Interest The authors declare that they have no conflict of interest.

Consent to Participate Not applicable.

Consent for Publication Not applicable.

References

1. Threadgilll PL, Leonard AJ, Shercliff HR, Withers PJ (2009) Friction stir welding of aluminium alloys. Int Mater Rev 54:49–93. https://doi.org/10.1179/174328009X411136
2. Khanna N, Sharma P, Bharati M, Badheka VJ (2020) Friction stir welding of dissimilar aluminium alloys AA 6061 – T6 and AA 8011 – h14: a novel study. J Brazilian Soc Mech Sci Eng 3:. https://doi.org/10.1007/s40430-019-2090-3
3. Palani K, Elanchezhian C, Avinash K, Karthik C, Chaitanya K, Sivanur K, Yugandhar Reddy K (2018) Influence of friction stir processing parameters on tensile properties and microstructure of dissimilar AA 8011-H24 and AA 6061-T6 aluminum alloy joints in nugget zone. IOP Conf Ser Mater Sci Eng 390:0–10. https://doi.org/10.1088/1757-899X/390/1/012108
4. Chandrasekar P, Natarajan S, Ramkumar KR (2019) Influence of carbide reinforcements on accumulative roll bonded Al 8011 composites. Mater Manuf Process 34:889–897. https://doi.org/10.1080/10426914.2019.1594279
5. Natrayan L, Kumar MS (2020) Optimization of wear behaviour on AA6061/Al2O3/SiC metal matrix composite using squeeze casting technique–Statistical analysis. Materials Today: Proceedings 27:306–310. https://doi.org/10.1016/j.matpr.2019.11.038
6. Stalin B, Ravichandran M, Marichamy S et al (2020) Friction welding parametric optimization of AISI 310L austenitic stainless steel weld joints-Grey relational investigation. AIP Conf Proc 2283:020141. https://doi.org/10.1063/5.0024979
7. Jacquin D, Guillemot G (2021) A review of microstructural changes occurring during FSW in aluminium alloys and their modelling. J Mater Process Technol 288:116706. https://doi.org/10.1016/j.jmatprotec.2020.116706
8. Prater T, Strauss A, Cook G, Gibson B, Cox C (2013) A comparative evaluation of the wear resistance of various tool materials in friction stir welding of metal matrix composites. J Mater Eng Perform 22:1807–1813. https://doi.org/10.1007/s11665-012-0468-9
9. Pan R, Zheng J, Zhang Z, Lin J (2019) Cold rolling influence on residual stresses evolution in heat-treated AA7xxx T-section panels. Mater Manuf Process 34:431–446. https://doi.org/10.1080/10426914.2018.1512121
10. Anand R, Sridhar VG (2020) Studies on process parameters and tool geometry selecting aspects of friction stir welding-a review. Mater Today Proc 27:576–583. https://doi.org/10.1016/j.matpr.2019.12.042
11. Kadlec M, Růžek R, Nováková L (2015) Mechanical behaviour of AA 7475 friction stir welds with the kissing bond defect. Int J Fatigue 74:7–19. https://doi.org/10.1016/j.ijfatigue.2014.12.011
12. Storjohann D, Barabash OM, Babu SS et al (2005) Fusion and friction stir welding of aluminum-metal-matrix composites. Metall Mater Trans A Phys Metall Mater Sci 36:3237–3247. https://doi.org/10.1007/s11661-005-0093-4
13. Kim YG, Fujii H, Tsumura T, Komazaki T, Nakata K (2006) Three defect types in friction stir welding of aluminum die casting alloy. Mater Sci Eng A 415:250–254. https://doi.org/10.1016/j.msea.2005.09.072
14. Natrayan L, Senthil Kumar M (2020) An integrated artificial neural network and Taguchi approach to optimize the squeeze cast process parameters of AA6061/Al2O3/SiC/Gr hybrid composites prepared by novel encapsulation feeding technique. Mater Today Commun 25:101586. https://doi.org/10.1016/j.mtcomm.2020.101586
15. Natrayan L, Senthil Kumar M (2020) Influence of silicon carbide on tribological behaviour of AA2024/Al2O3/SiC/Gr hybrid metal matrix squeeze cast composite using Taguchi technique. Mater Res Express 6:1265f9. https://doi.org/10.1088/2053-1591/ab676d
16. Senthil Kumar M, Mangalaraja RV, Senthil Kumar R, Natrayan L (2019) Processing and characterization of AA2024/Al2O3/SiC reinforces hybrid composites using squeeze casting technique. Iran J Mater Sci Eng 16:55–67. https://doi.org/10.22068/ijmse.16.2.55
17. Jafari H, Mansouri H, Honarpisheh M (2019) Investigation of residual stress distribution of dissimilar Al-7075-T6 and Al-6061-T6 in the friction stir welding process strengthened with SiO2 nanoparticles. J Manuf Process 43:145–153. https://doi.org/10.1016/j.jmapro.2019.05.023
18. Anand R, Sridhar VG (2020) Effects of SiC and Al2O3 Reinforcement of Varied Volume Fractions on Mechanical and Micro Structure Properties of Interlock FSW Dissimilar Joints AA7075-T6-AA7475-T7. Silicon 1–13. https://doi.org/10.1007/s12633-020-00630-y
19. Bharathi SRS, Rajeshkumar R, Rose AR, Balasubramanian V (2018) Mechanical properties and microstructural characteristics of friction welded dissimilar joints of aluminium alloys. Trans Indian Inst Metals 71:91–97. https://doi.org/10.1007/s12666-017-1143-5
20. Bhushan RK, Sharma D (2020) Optimization of parameters for maximum tensile strength of friction stir welded AA6082/Si3N4 and AA6082/SiC composite joints. Silicon 12:1195–1209. https://doi.org/10.1007/s12633-019-00216-3
21. Qin Q, Zhao H, Zhang Y, Li J, Wang Z (2019) Microstructures and mechanical properties of Al-Mg2Si-Si alloys resistance spot welded with Al-Si interlayers. J Mater Res Technol 8:4318–4332. https://doi.org/10.1016/j.jmrt.2019.07.043
22. Hemanth RD et al (2017) Evaluation of mechanical properties of e-glass and coconut fiber reinforced with polyester and epoxy resin matrices. Intern J of Mech Prod Eng Res Dev 7(5):13–20
23. Abioye TE, Zuhailawati H, Anasyida AS, Yahaya SA, Dhindaw BK (2019) Investigation of the microstructure, mechanical and wear properties of AA6061-T6 friction stir weldments with different particulate reinforcements addition. J Mater Res Technol 8:3917–3928. https://doi.org/10.1016/j.jmrt.2019.06.055
24. Xu W, Liu J, Luan G, Dong C (2009) Microstructure and mechanical properties of friction stir welded joints in 2219-T6 aluminum alloy. Mater Des 30:3460–3467. https://doi.org/10.1016/j.matdes.2009.03.018
25. Kar A, Kailas SV, Suwas S (2018) Effect of zinc interlayer in microstructure evolution and mechanical properties in dissimilar friction stir welding of aluminum to titanium. J Mater Eng Perform 27:6016–6026. https://doi.org/10.1007/s11665-018-3697-8

26. Suresh S, Venkatesan K, Natarajan E (2018) Influence of SiC nanoparticle reinforcement on FSS welded 6061-T6 aluminum alloy. J Nanomater 2018:1–11. https://doi.org/10.1155/2018/7031867
27. Sagheer-abbasi Y (2019) Optimization of parameters for micro friction stir welding of aluminum 5052 using Taguchi technique. Int J Adv Manuf Technol 102(1–4):369–378
28. Sachinkumar, Narendranath S, Chakradhar D (2019) Microstructure, hardness and tensile properties of friction stir welded aluminum matrix composite reinforced with SiC and fly ash. Silicon 11:2557–2565. https://doi.org/10.1007/s12633-018-0044-5
29. Natrayan L, Senthil kumar M, Palanikumar K (2018) Optimization of squeeze cast process parameters on mechanical properties of Al2O3/SiC reinforced hybrid metal matrix composites using taguchi technique. Mater Res Expr 5(6):066516
30. Mokabberi SR, Movahedi M, Kokabi AH (2018) Effect of interlayers on softening of aluminum friction stir welds. Mater Sci Eng A 727:1–10. https://doi.org/10.1016/j.msea.2018.04.093
31. Aleem Pasha M, Ravinder Reddy P, Laxminarayana P, Khan IA (2019) SiC and Al2O3 reinforced friction stir welded joint of aluminium alloy 6061. Strengthening and Joining by Plastic Deformation, pp 163–182. https://doi.org/10.1007/978-981-13-0378-4_7
32. Humphreys FJ, Hatherly M (2004) Grain growth following recrystallization. Recryst Relat Annealing Phenom 333–378. https://doi.org/10.1016/b978-008044164-1/50015-3
33. Abu-Okail M, Abu-Oqail A, Ata MH (2020) Effect of friction stir welding process parameters with interlayer strip on microstructural characterization and mechanical properties. J Fail Anal Prev 20:173–183. https://doi.org/10.1007/s11668-020-00813-0
34. Singh A, Kumar V, Grover NK (2019) A study of microstructure and mechanical properties of friction stir welding aluminium alloy AA6082 with Zn interlayer. Mater Res Express 6:0–10. https://doi.org/10.1088/2053-1591/ab4b1f
35. Tan S, Zheng F, Chen J, Han J, Wu Y, Peng L (2017) Effects of process parameters on microstructure and mechanical properties of friction stir lap linear welded 6061 aluminum alloy to NZ30K magnesium alloy. J Magnes Alloy 5:56–63. https://doi.org/10.1016/j.jma.2016.11.005
36. Hamdollahzadeh A, Bahrami M, Farahmand Nikoo M, Yusefi A, Besharati Givi MK, Parvin N (2015) Microstructure evolutions and mechanical properties of nano-SiC-fortified AA7075 friction stir weldment: the role of second pass processing. J Manuf Process 20:367–373. https://doi.org/10.1016/j.jmapro.2015.06.017
37. Yogeshwaran S et al (2015) Mechanical properties of leaf ashes reinforced aluminum alloy metal matrix composites. Int J Appl Eng Res 10(13):11048–11052